JOURNAL OF SOLID STATE CHEMISTRY 41, 233–243 (1982)

An Electron Microscope Study of the Rhombohedral Phase Occurring in The Bi_2O_3–BaO System

R. J. D. TILLEY

School of Materials Science, University of Bradford, Bradford, West Yorkshire BD7 1DP, England

Received May 4, 1981; in revised form August 24, 1981

The rhombohedral phase which occurs at about 20 mole% BaO in the Bi_2O_3–BaO system has been studied by electron microscopy. While some material seems identical to that found by X-ray diffraction, many crystals show the existence of a superlattice on the electron diffraction patterns. This superlattice is believed to arise as a result of ordering of the Bi and Ba atoms in the structure. Electron micrographs suggest that the ordered regions are small and can be regarded as microdomains within the parent crystal matrix.

Introduction

Some 40 years ago Aurivillius and Sillén discovered that a number of grossly nonstoichiometric phases formed when Bi_2O_3 was reacted with a number of divalent metal oxides (*1–5*). Much later, Levin and Roth (*6*) made a systematic study of the phase region close to Bi_2O_3 for a number of *M*–Bi–O ternary systems. Their work confirmed that grossly nonstoichiometric oxides readily formed in such systems. The broad stoichiometry ranges of these materials is of considerable interest, and structural studies of these oxides would be expected to provide some new insights into the manner in which oxides are able to accommodate changes in anion to cation ratio. Although X-ray structure determinations are of prime importance here, studies over the last 10 years or so have shown that considerable information is provided by high-resolution electron microscopy, in conjunction with a lower-resolution phase-analytical technique such as powder X-ray diffraction. With this in mind we have commenced an electron microscope study of the ternary bismuth oxides. This communication describes the first of these studies, and is concerned with the rhombohedral phase formed by reacting Bi_2O_3 with BaO in air.

The rhombohedral phase in the Bi_2O_3–BaO system was first discovered by Aurivillius (*4*) and would appear to be isostructural with simlar phases in the CaO–Bi_2O_3, SrO–Bi_2O_3, Sm_2O_3–Bi_2O_3, and La_2O_3–Bi_2O_3 systems (*6*). The phase range was estimated as 10–22 at.% Ba by Aurivillius (*4*) and as 20–25 mole% BaO by Takahashi *et al.* (*7*). No structural work has been carried out on this compound except for its lattice parameter determination which is given by Levin and Roth as a_0 = 0.9786 nm, $\alpha = 23°26'$ for the rhombohedral cell, which is equivalent to a_0 = 0.3972 nm, c_0 = 2.854 nm in terms of hexagonal axes, for the phase coexisting with Bi_2O_3 at about

0022-4596/82/030233-11$02.00/0

973 K. The lattice parameter does, of course, vary with composition. While further structural information is not available it is reasonable to assume that it is fairly similar in structure to the rhombohedral phase formed in the $SrO-Bi_2O_3$ system, which was originally solved by Aurivillius (*4*) and confirmed by a recent structural determination on rhombohedral $Sr_{0.235}Bi_{0.765}O_{1.383}$ by Conflant *et al.* (*8*). In this report we present the preliminary results of an electron microscope study of the rhombohedral phase in the $BaO-Bi_2O_3$ system.

Experimental

All samples were prepared from Bi_2O_3 and $BaCO_3$ of specpure grade, supplied by Johnson Matthey Chemicals Ltd., following the method of Aurivillius (*4*). Known weights of Bi_2O_3 and $BaCO_3$ to yield samples of overall Ba:(Ba + Bi) ratios of 10, 15, and 20% corresponding to 18, 26, and 33 mole% BaO were ground together in an agate mortar and then heated in small platinum vessels. The temperature of the furnace was increased slowly from room temperature to 1173 K to allow for the controlled decomposition of the $BaCO_3$. The samples were then held at 1173 K, at which temperature they were molten, for 30 min. They were then either air-quenched, by rapidly pulling them from the furnace, or else they were annealed at 723 K for 60 or 1000 hr.

All samples were examined by optical microscopy, electron microscopy and X-ray diffraction. Powder X-ray photographs were taken using a Guinier–Hägg focusing camera using strictly monochromatic Cu$K\alpha_1$ radiation and KCl (a_0 = 0.62919 nm) as an internal standard. Film measurements were refined by least-squares techniques. Samples were examined optically using a Zeiss Ultraphot microscope. Transmission electron microscopy was undertaken using a JEM 100B electron microscope fitted with a goniometer stage and operated at 100 kV. Electron microscope samples were prepared by crushing crystals in an agate mortar under *n*-butanol; a drop of the resultant suspension being allowed to dry on a holey carbon film.

Results

The X-ray powder patterns of the air-quenched materials showed only a single phase over the whole of the composition range examined. The diffraction lines were broad and poorly defined, a feature which became more pronounced as the Ba content increased. The lines could all be indexed in terms of a rhombohedral unit cell, and comparison with data in the literature showed that the material was the rhombohedral solid solution phase of Aurivillius (*4*).

Annealing these samples for 60 hr at 723 K produced little change in the appearance of these X-ray lines. Indeed, if anything the lines were slightly more diffuse. The 15 and 20 cation% samples showed no new lines after this treatment, but the 10 cation% sample was now found to contain a fair amount of the monoclinic form of Bi_2O_3. It was notable that the lines of the Bi_2O_3 were sharp, in contrast to those of the rhombohedral phase.

The samples annealed for 1000 hr again showed little change in the appearance of the rhombohedral phase lines, which were still similar to lines on the air quenched films. All films now contained lines from phases other than the rhombohedral material. The 10 cation% sample contained a good deal of monoclinic Bi_2O_3, and a trace of this phase was found in the 15 cation% sample. The 20 cation% sample showed, in addition to the rhombohedral phase, a sharp set of lines which were from a tetragonal phase.

The lattice parameter of the rhombohe-

FIG. 1. X-Ray film of the rhombohedral phase formed at 15 at.% Ba in the $BaO–Bi_2O_3$ system. The sample has been annealed for 60 hr at 723 K. The broadness of the lines is noticeable when compared with the lines from the KCl standard, which are marked with spots.

dral phase was calculated from a film of the 15 cation% material annealed for 60 hr. The film is shown in Fig. 1, which reveals the broadness of the X-ray reflections. The lattice parameters, obtained using least squares refinement techniques, were found to be $a_0 = 0.97_7$ nm, $\alpha = 23.83°$ which is equivalent to $a_0 = 0.399$ nm, $c_0 = 2.847$ nm in terms of hexagonal indices. These are in good agreement with those listed by Levin and Roth (*6*) for this material, *viz.*, $a_0 = 0.978_6$ nm, $\alpha = 23.43°$, ($a_0 = 0.397_2$ nm, $c_0 = 2.854$ nm for the hexagonal cell) when the broadness of the X-ray reflections are considered.

Optical microscopy revealed the platey nature of the crystals; something which was confirmed by noting their micaceous behaviour on grinding in an agate mortar. Electron microscopy also showed this clearly. Large sheets of thin crystals were often located, which showed extensive dislocation arrays and Moiré patterns where thin areas of the crystal flake were displaced one with another. Figure 2 shows a typical crystal flake, which shows similar contrast to graphite, V_2O_5 and other platey materials which have been examined electron optically.

Electron diffraction patterns showed that the crystal plates were (00.1) plates, rereferred to the hexagonal unit cell, and hexagonal arrays of spots, corresponding to the (00.1) zone were obtained on tilting the crystals by only small amounts.[1] An example is shown in Fig. 3a. Measurement of these diffraction patterns allowed the indices indicated on Fig. 3a to be assigned to the reflections. It is apparent, though, that these reflections do not obey the extinctions associated with a rhombohedral space group but conform to a hexagonal symme-

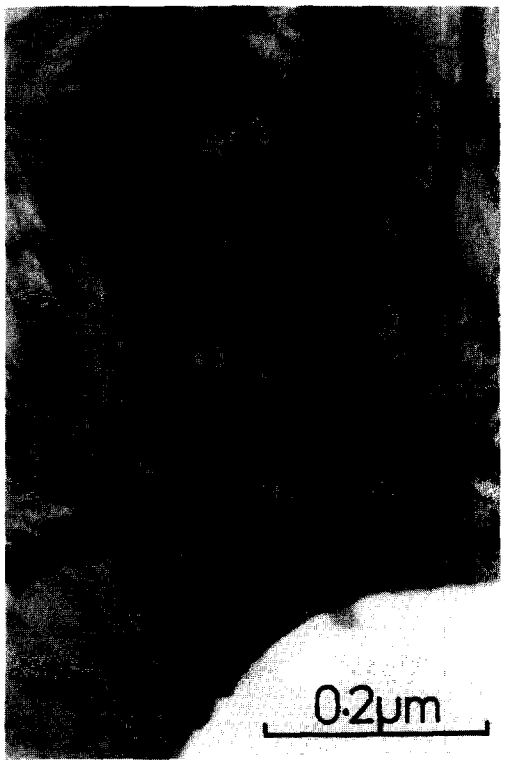

FIG. 2. Low-magnification electron micrograph of a typical crystal plate of the rhombohedral phase. The dark bands are extinction contours and indicate that the plate is bowed into either a saucer or a dome shape.

[1] All indices are referred to the hexagonal unit cell throughout the paper.

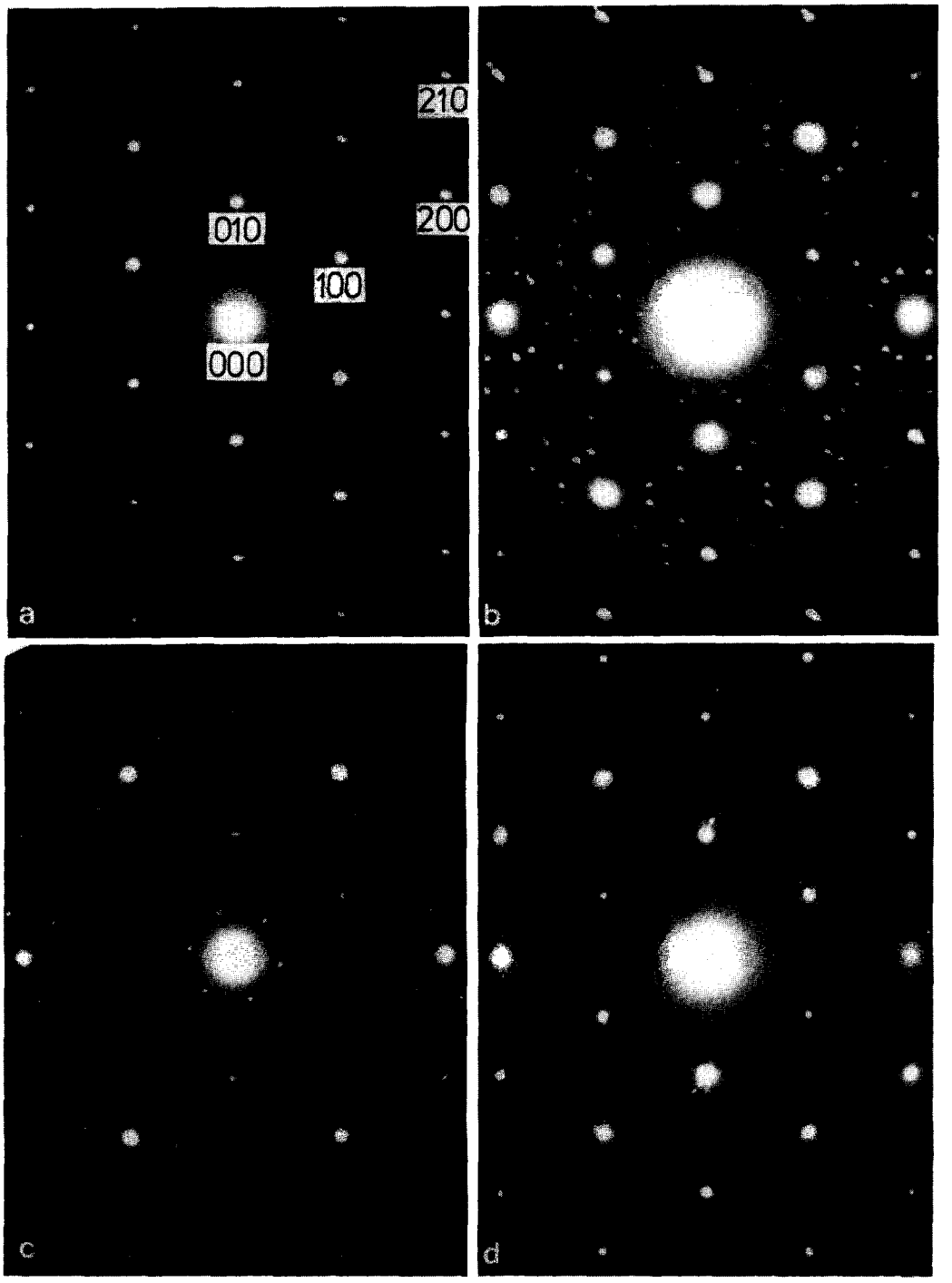

FIG. 3. Diffraction patterns from the rhombohedral phase. (a) Diffraction pattern corresponding to the X-ray unit cell. The indices refer to hexagonal axes. (b) Typical superlattice pattern, (c) rarely encountered superlattice pattern. The circle of intensity is an artifact due to disordered material also included within the region contributing to the diffraction pattern, (d) diffraction pattern showing faint regions of diffuse scattering.

try. In reality, such simple patterns were only rarely encountered in this study and it was found that a superlattice often occurred on diffraction patterns. These superlattice spots were seen on crystal fragments taken from all samples; that is, from air-quenched as well as annealed materials. However, not every crystal fragment showed such superlattice spots, and the intensity of the superlattice varied a great deal. Figure 3b shows a typical example. The superlattice array shown in Fig. 3c was more rarely found, and only when diffraction patterns from rather small volumes of crystal were considered. Using a larger aperture, or displacing the crystal slightly would invariably change a pattern of the type shown in Fig. 3c into that shown in Fig. 3b. Very rarely indeed, a few patches of diffuse intensity were seen at places on the diffraction pattern where the sharp superlattice spots ultimately appeared. This effect is shown in Fig. 3d.

In order to determine the origin of the superlattice spots a number of imaging techniques were tried. Dark-field studies were unsuccessful because the intensities of the reflections were too weak for reasonable micrographs to be produced. High-resolution imaging was difficult, as many crystal flakes decomposed under the influence of the electron beam. However, by working at as low an intensity of illumination as possible, reasonable micrographs could be obtained. In general, an objective aperture was used which allowed the six subcell spots to contribute to the image as well as the superlattice spots. Typical examples are shown in Figs. 4 and 5.

In these micrographs a number of features are revealed. The major contrast effect is a set of fringes with a spacing of 0.34 nm. These form a general background over the crystal flakes and correspond to the hexagonal (100) spacings formed by subcell spots of the type shown on Fig. 3a. In some parts of the crystal only one set of fringes appear, while in other areas two or more sets are seen. These effects are due to the varying thickness and orientation of the crystal fragments and are not significant chemically. These subcell fringes are shown on the lower part of Fig. 4 and in the background in Fig. 5.

Superimposed upon these fringes are a rather ill-defined wider set, shown in the upper part of Fig. 4 and in a number of regions of Fig. 5. The spacing of these fringes, about 0.9 nm, suggests that they arise from the superlattice reflections. This is confirmed by measuring the angles between these wider fringes and the subcell fringes. In all cases these angles correspond

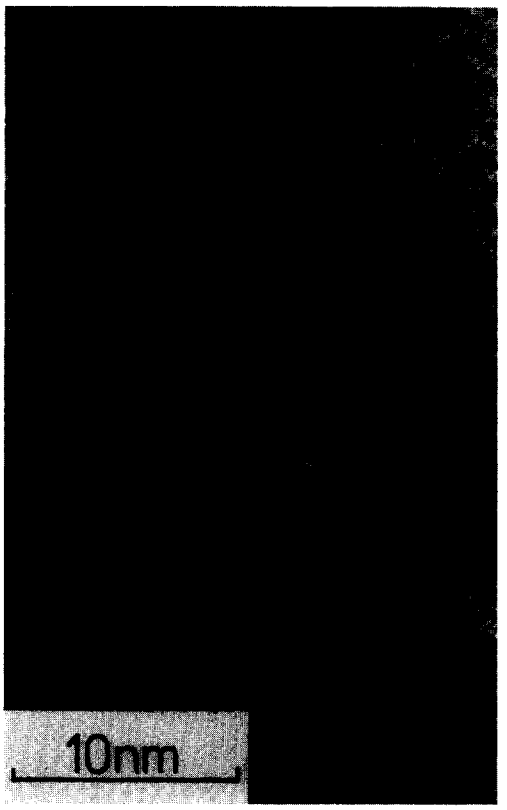

FIG. 4. Electron micrograph of a crystal fragment of the rhombohedral phase. On the lower left of the figure the (100) fringes (0.34 nm) of the hexagonal subcell are seen, while on the upper right superlattice fringes (0.9 nm) are superimposed on them.

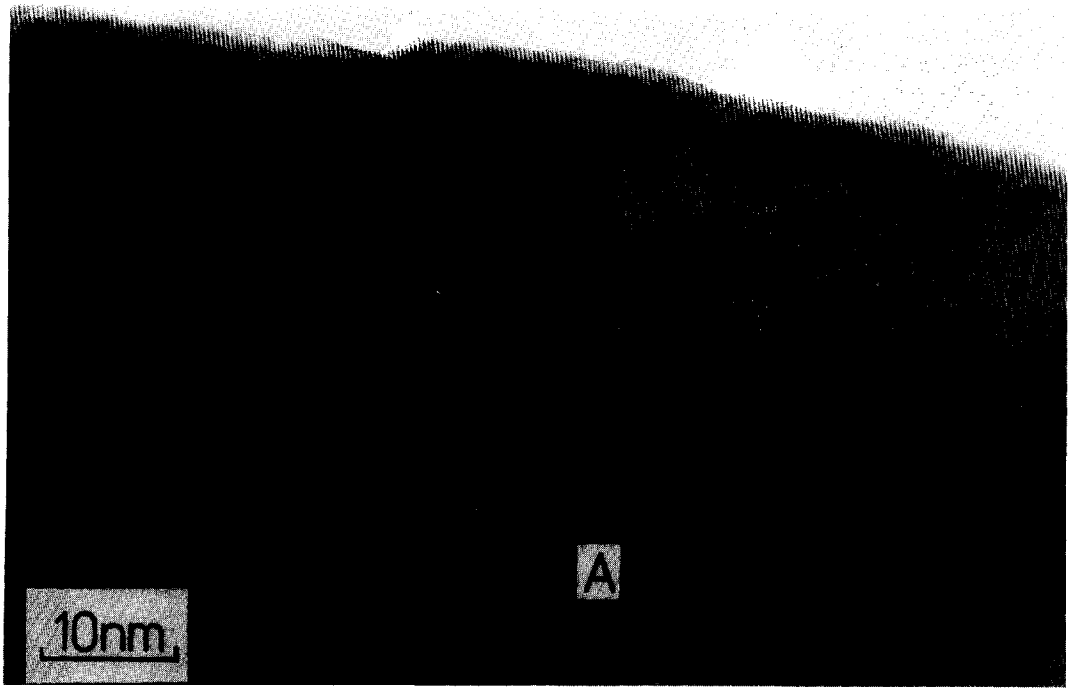

FIG. 5. Typical crystal fragment of the rhombohedral phase. In the background (100) fringes (0.34 nm) of the hexagonal subcell are resolved while in other regions wider fringes (0.9 nm) characteristic of the superlattice are superimposed on the sublattice set. A variety of superlattice fringe directions are seen and in some areas, labeled A, two sets overlap.

to the angles between the superlattice reflections and the subcell reflections on the diffraction patterns which contain both sets of spots. As with the subcell fringes, sometimes only one set occur while at other times at least two overlapping sets arise in the same volume of crystal.

Interpretation and Discussion

The X-ray powder patterns of the rhombohedral phase are interesting because of the broadness of the lines, and particularly because the lines do not sharpen as the samples are annealed. The usual interpretation of such broad lines is in terms of small particle size effects. Here, though, this will not hold, as the crystals are large, often being above 1 mm diameter, and in an optical microscope do not show signs of being composed of an oriented array of microcrystallites. The degree of line broadening also increases with Ba content, indicating that the nonstoichiometric structure of the crystals is somehow involved. The simplest interpretation of this behavior is to assume that the nonstoichiometry is accommodated structurally into the apparently single crystals in a way which leads to small particle diffraction effects. We are thus lead to consider that a microdomain model holds, in which we have regions of ordered structure which are out of phase with each other as we move from one part of the crystal to another (*9*). The fact that optically the crystals appear perfect implies that some important part of the crystal structure must remain unchanged as we pass from one microdomain to another. In oxides this is usually taken to be the oxygen array, but

other possibilities exist. As microdomains appear to be relatively stable in systems which prefer them, the fact that the X-ray patterns do not change on annealing is not unexpected and in agreement with the experimental evidence.

In terms of a qualitative explanation, the electron diffraction patterns present little problem. In those patterns which display only bright hexagonal subcell reflections we are detecting the information usually found by X-ray diffraction. Thus the diffraction pattern shown in Fig. 3a could be indexed completely in terms of the original X-ray data of Aurivillius (*4*) with the indices referred to the hexagonal unit cell of this phase. However, for true rhombohedral symmetry many of these reflections should be absent; the first $h00$ type of reflection which should occur being 300, for example.

There are a number of explanations for this observation. Certainly it is possible that the true symmetry of the phase is hexagonal rather than rhombohedral, but the X-ray powder data support a rhombohedral symmetry and we assume that this assignment is correct. The presence of the forbidden reflections must then be attributed to the dynamical nature of the electron diffration. Appreciable intensities for forbidden reflections can occur by a number of mechanisms. In our case the very platey nature of the crystals suggests that double diffraction is responsible, and, in fact, forbidden reflections are frequently observed in the diffraction patterns of other crystals of similar plate-like morphology. This problem is therefore regarded as one of diffraction physics rather than chemistry, and will not be taken further here.

The two superlattice patterns illustrated in Figs. 3b and c cannot, though, be explained in terms of the X-ray data. A brief inspection of these patterns shows that in this case the extra spots are not due to double diffraction effects or to the appearance of forbidden reflections which normally have zero intensity. The extra spots are therefore due to some additional ordering within the structure, over and above that detected by the X-ray studies. The high symmetry of the diffraction patterns of the type shown in Fig. 3b was suggestive of twinning, and the discovery of the simpler superlattice type, shown in Fig. 3c confirmed this. This latter pattern was the simplest one found, and we presume that it represents the real reciprocal lattice of the superlattice and not a twinned form. It is drawn out for clarity in Fig. 6. Twinning about (110) will double the number of spots present, and reproduces the pattern of reflections shown in Fig. 3b, as is illustrated in Fig. 6.

In electron microscopy it is usually a simple matter to detect twinning in a crystal by detecting electron diffraction contrast from twin boundaries, which is characteristic and has been well documented in the past (*10*). One of the interesting features of the present investigation was that twin boundaries were never noticed on crystal fragments examined by normal diffraction contrast techniques. Careful searching for this, or related, contrast effects, which included tilting crystals well away from the basal projections shown above, was completely unsuccessful. This suggests that the twins, if they exist, are small in dimension, which brings us once more toward the microdomain concept.

The high-resolution electron micrographs are in support of this model. As shown in Figs. 4 and 5 some regions of a crystal flake show only the fringes characteristic of the (100) subcell reflections while in other closely adjacent regions, the wider fringes of the superlattice appears. Crystal fragments often appear as mosaics of regions showing only subcell fringes, regions with only one set of superlattice fringes, and other regions where two sets of superlattice fringes clearly overlap. The interpretation of these contrast effects is consistent with a

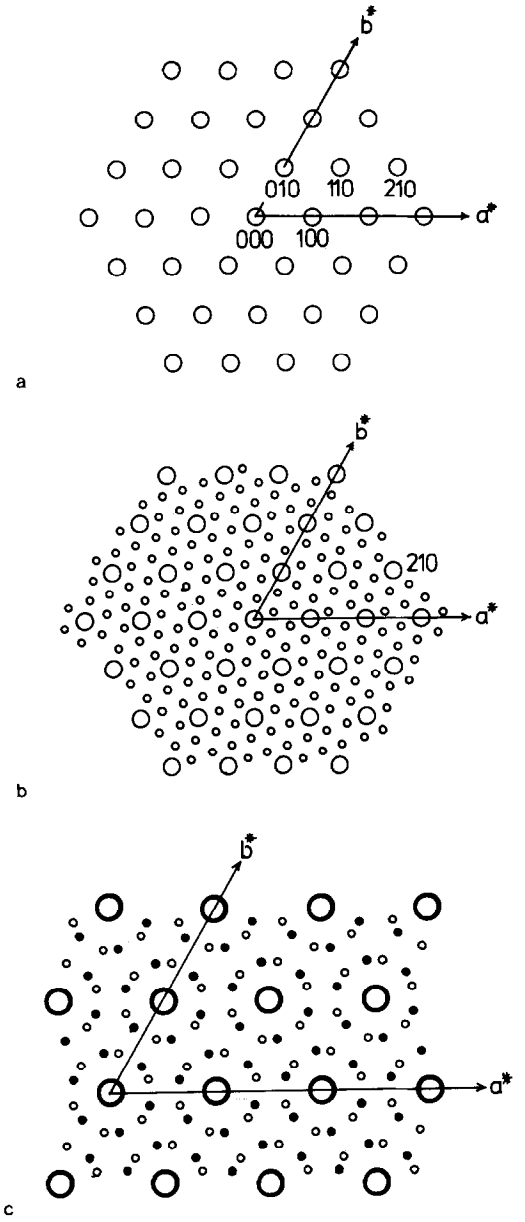

FIG. 6. (a) Drawing of the basal plane of the rhombohedral phase reciprocal lattice. The indices refer to the hexagonal unit cell. This drawing is equivalent to Fig. 3a. (b) The same reciprocal lattice section as in (a) but with the superlattice spots of the type shown in Fig. 3c included. (c) An enlarged drawing of part of (b) showing the extra spots (filled circles) generated by twinning about the [110] direction. It is seen that this pattern is identical to the diffraction pattern shown in Fig. 3b.

model in which we have microdomains of ordering within the matrix of a normally disordered phase. The size of these domains varies widely, but single-domain crystal flakes have not been observed in our study, and this suggests that true single crystals, in the X-ay sense, will be hard to prepare. The absence of pronounced boundary effects between microdomains indicates that we do not have a phase separation in the classical sense and that the changes in the atomic arrangements as we go from one domain to another must be small.

The final question to consider is the origin of the superlattice and structural nature of the microdomains. The presence of the superlattice implies that some additional ordering is taking place within the structure in addition to that required for the production of the X-ray unit cell. There are two possibilities for this ordering. In terms of the nonstoichiometry, the most likely candidates for ordering are the unoccupied oxygen sites or oxygen "vacancies" as they are sometimes labeled. This idea is attractive as we know that such a set of unoccupied positions exists in the strontium analogue of the rhombohedral phase However, the intensity scattered by oxygen atoms will, in general, be low, and while the superlattice reflections recorded here are much lower than the matrix reflections, they are still appreciable.

An alternative possibility is that there is an ordering of the barium and bismuth cations in the structure. The problem is to try to devise an ordering pattern which will generate the observed superlattice without a knowledge of the basic structure of the phase. It is reasonable, once again, to turn to the structure of the rhombohedral phase in the strontium–bismuth–oxygen system for guidance. If we assume that the major features of this structure can be taken to hold in the barium–bismuth oxide studied here, then we can sketch out a simplified

version of the structure, as shown in Fig. 7. It is seen that the structure is composed of lamellae stacked parallel to the hexagonal c axis and that in each lamella, only the middle layer of atoms contains both bismuth and barium. If these atoms are ordered it will give rise to a superlattice. We will suppose that this is so for the moment.

An examination of the superlattice, which is drawn out in Fig. 6, shows that the shortest reciprocal lattice spacing, which is the longest spacing in the real structure, is seven times the d_{210} spacing and in a direction normal to the (210) planes, as the region of space on the diffraction pattern between the 210 spot and the origin is subdivided by six superlattice spots. Assuming that the cations in the barium–bismuth sheet are arranged in a hexagonal array, as they are in the strontium oxide, we can place, say, a barium atom at the origin and then another at the available position 7 $\times$ d_{210} away from it in a direction normal to the (210) plane. Examination of the diagram shown as Fig. 8 reveals that there is no cation site at this spot, but that there is a suitable position at 14 $\times$ d_{210} from the origin. We assume that a second barium then occupies this site. We can proceed along the other axis of the superlattice, to the $\bar{1}30$ reflection, and again place a barium atom in the metal atom position which is 14 $\times$ d_{210} from the origin.

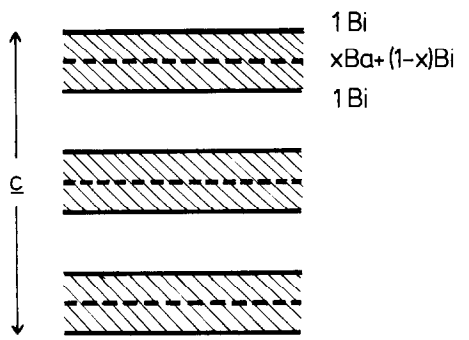

FIG. 7. Schematic illustration of the probable structure of the rhombohedral phase in the BaO–Bi_2O_3 system. Each layer of the structure contains three atom planes, only the middle of which is populated by both Ba and Bi atoms. Each plane also contains oxygen atoms. The hexagonal c axis is normal to the layers. Within each atom plane the metal atoms are arranged in a hexagonal array.

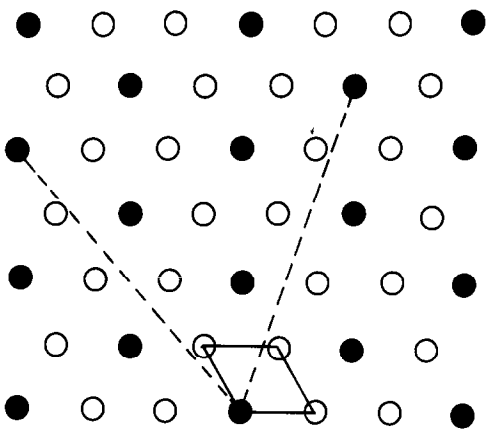

FIG. 8. Schematic illustration of the atom arrangement which could give rise to the superlattice reflections shown in Fig. 3. The empty circles represent Bi atoms and the filled circles Ba atoms. The sheet of atoms represented is projected normal to the hexagonal c axis and the hexagonal unit cell is outlined. The broken lines are normal to the (120) and the equivalent $(\bar{1}30)$ planes and of a length equal to 14 $\times$ d_{120}.

In order to progress further it is necessary to obtain an estimate of the ratio of barium atoms to bismuth atoms in the mixed cation layers. We can do this by considering the overall composition of the rhombohedral phase. This is given by Takahashi *et al.* (*7*) as from 20 to 25 mole% BaO, which is somewhat narrower than the composition range given by Aurivillius (*4*). Taking the narrower range, and referring to the cation distribution indicated in Fig. 8, we see that for every 1 Ba atom we must have 8 Bi atoms in the 20 mole% BaO case and 6 Bi atoms in the 25 mole% BaO case. As each layer of the structure contains three cations, two of which are Bi, the makeup of the middle mixed layer must be $\frac{1}{3}$ Ba : $\frac{2}{3}$ Bi for the 20 mole% BaO case and 0.43 Ba to 0.57 Bi for the 25 mole% BaO. It

is clearly simpler to work with a $\frac{1}{3}:\frac{2}{3}$ ratio, and using these proportions we have filled up the atom positions in an ordered fashion as shown in Fig. 8.

This type of arrangement accounts for the superlattice spots in a qualitative fashion. The twinning seen is easily reproduced by altering the arrangement of barium and bismuth sites. Such a structural model also explains the contrast observed on the micrographs. In some regions the cations will be disordered, and no superlattice fringes will be observed. If a degree of short-range order exists between these cations it will give rise to diffuse scattering, which will gradually condense into sharp reflections as the degree of ordering increases. This type of effect is shown in Fig. 3d. In regions where an ordered arrangement like that shown in Fig. 8 is found a single set of superlattice fringes will be produced. In some parts of the crystals it is seen that the twinning of the superlattice occurs even within small domains. Here we suppose that although the ordering pattern in each layer of the structure is as shown, the layers when stacked on top of one another, are not in perfect register as far as the cation distributions in the layers are concerned. This will give rise to the microtwinned domains observed. We can also note that the various arrangements or ordered domains also allow for a variation in the barium to bismuth stoichiometry of the material, without recourse to any disorder. When a twin boundary forms, or when two ordered domains meet, the overall stoichiometry will change from the $\frac{1}{3}:\frac{2}{3}$ ratio of the domain center. The change in stoichiometry will depend upon the nature of the boundary region between the domains. We will not illustrate this effect here, but note that Roth (*12*) has described an analogous situation for microdomains in β-alumina-type compounds which is directly applicable to the situation pertaining here. It must finally be stressed, though, that this structural model must be regarded as hypothetical until calculations have been made to verify it. Such calculations will form part of a future program of study.

One feature of interest is that the form of the superlattice does not change over the whole of the composition range in question. This implies that the ordering pattern that produces the superlattice does not evolve as the stoichiometry changes across the composition range of the rhombohedral phase. This obervation is in accord with the microdomain model suggested above. In addition, the superlattice does not change with annealing time, although crystal fragments which show the superlattice are not so common in the air-quenched samples. This suggests that the ordering is fairly rapid, but the occasional observations of diffuse scattering in the places where superlattice spots develop show that the ordering process takes place within an accessible time scale. A study of rapidly quenched material, followed by short anneals should reveal the ordering process in more detail.

Finally, we should note that although a careful study of these samples was made electron optically, no indication of planar faults were found which could be associated with the variation in stoichiometry in the rhombohedral phase. This is not surprising. The parent oxide Bi_2O_3 has a structure related to the fluorite structure type (*13*), which is not amenable to the incorporation of planar faults such as crystallographic shear planes to accommodate stoichiometric variation (*14*).

References

1. L. G. SILLÉN, *Ark. Kemi Mineral. Geol. A* **12**(18), 1 (1937).
2. L. G. SILLÉN AND B. AURIVILLIUS, *Z. Kristallogr.* **101**, 483 (1939).
3. L. G. SILLÉN AND B. SILLÉN, *Z. Phys. Chem. B* **49**, 27 (1941).

4. B. AURIVILLIUS, *Ark. Kemi Mineral. Geol. A* **16**(17), 1 (1943).
5. B. AURIVILLIUS AND L. G. SILLÉN, *Nature* **155**, 305 (1945).
6. E. M. LEVIN AND R. S. ROTH, *J. Res. Nat. Bureau Standards Sect. A* **68**, 197 (1964).
7. T. TAKAHASHI, T. ESAKA, AND H. IWAHARA, *J. Solid State Chem.* **16**, 317 (1976).
8. P. CONFLANT, J-C. BOIVIN, AND D. THOMAS, *J. Solid State Chem.* **35**, 192 (1980).
9. J. S. ANDERSON, *in* "Problems of Nonstoichiometry" (A. N. Rabenau, Ed.), North-Holland, Amsterdam (1970).
10. S. AMELINCEX, *Surface Sci.* **31**, 296 (1972).
11. P. B. HIRSCH, A. HOWIE, R. B. NICHOLSON, D. W. PASHLEY, AND M. J. WHELAN, "Electron Microscopy of Thin Crystals." Butterworths, London (1965), [particularly Chaps. 5, 6, 15].
12. R. S. ROTH, *J. Solid State Chem.* **4**, 60 (1972).
13. H. A. HARWIG, *Z. Anorg. Allgem. Chem.* **444**, 151 (1978).
14. B. G. HYDE, *Nature* **250**, 411 (1974).